A Numerical Investigation of TBA.....!!!1

By H.G.K.G Jayatunga

A thesis submitted to Monash University in fulfilment of the requirements for the Degree of

Doctor of Philosophy

Department of Mechanical Engineering
Monash University
Date ...!!!!!!

Contents

Chapter 1

Governing parameters of fluid-elastic galloping

1.1 Introduction

This chapter contains the formulation of non dimensional governing parameters namely, the combined mass-stiffness Π_1 and the combined mass-damping Π_2 and the results and discussion demonstrating the influence of them. These parameters are formulated by obtaining the relevant time-scales of the system followed by non-dimesnionlising the governing QSS oscillator equation.

A comparison of Quasi-steady state data presented using the classical VIV parameters and the newly formulated Π_1 and $\Pi_2$is presented and it is concluded that $\Pi_2$provides a better collapse for velocity amplitude and mean power compared the classical reduced velocity (U^*) particularly because unlike U^*, Π_2 does not include a frequency component in it. This is followed by the presentation of QSS data and discussion on the influence of Π_1 and Π_2 on power, which concludes that the power transfer is a primary function of Π_2 and a weak function of Π_1.

Following this, a comparison of the QSS data with Direct Numerical Simulations (DNS) is presented. This reveals that the power transfer of the DNS data is strongly influenced by both Π_1 and Π_2. Further analysis reveals that there is a good agreement between QSS and DNS for velocity and power at substantially high Π_1Às Π_1 decreases, the deviation

(between QSS simulations and DNS) increases. Power spectral analysis of the DNS data shows a significant response at the vortex shedding at low Π_1. The relative strength was found out to be an inverse function of Π_1, which provides a clear explanation for the deviation between QSS simulations and DNS data at low Π_1. This is primarily due to the influence of vortex shedding where this effect is not accounted in the QSS model.

1.2 Formulation of the non-dimensionalised parameters Π_1 and Π_2

The natural time scales of the system could be obtained by linearising the quasi-steady equation of motion. (Eq: ***KJ: equation of motion ***) and finding the eigenvalues. The non-linear terms of the forcing function are truncated and the equation of motion could be expressed as,

$$m\ddot{y}+c\dot{y}+ky=\frac{1}{2}\rho U^2 \mathcal{A} a_1 \left(\frac{\dot{y}}{U}\right), \tag{1.1}$$

After combining the $\dot{y}$ terms and solving for eigenvalues the following solutions for the eigenvalues could be obtained.

$$\lambda_{1,2} = -\frac{1}{2}\frac{c-\frac{1}{2}\rho U \mathcal{A} a_1}{m} \pm \frac{1}{2}\sqrt{\left[\frac{c-\frac{1}{2}\rho U \mathcal{A} a_1}{(m)}\right]^2 - 4\frac{k}{m}}. \tag{1.2}$$

Galloping essentially occurs at low frequencies therefore it can be assumed that the spring is relevantly weak and therefore, $k \to 0$. Hence a single non-zero eigenvalue remains which is,

$$\lambda = -\frac{c-\frac{1}{2}\rho U \mathcal{A} a_1}{m}. \tag{1.3}$$

Further, if it is assumed that the mechanical damping is weaker than the fluid dynamic forces on the body the non zero eigenvalue could be further simplified to,

$$\lambda = \frac{\frac{1}{2}\rho U \mathcal{A} a_1}{m}. \tag{1.4}$$

In this representation λ represents the inverse time scale of the motion of the body due to the effect of long-time fluid dynamic forces (or forced due to the induced velocity). This term could also be re-written and λ could be expressed as

$$\lambda = \frac{a_1}{m^*}\frac{U}{D} \tag{1.5}$$

This form clearly shows the significant parameters that influences the inverse time scale of the system. $\partial C_Y/\partial\alpha$, the rate of change in the fluid dynamic force on the body, with respect to the induced angle of attack, is represented by a_1. $\frac{U}{D}$ represents the inverse advective time scale of the incoming flow, and the mass ratio is resented by m^*. Increasing a_1 would result in a rapid change of the fluid dynamic force with a small change of the induced angle θ, which is proportional to transverse velocity $\dot{y}$. It can be seen in equation 1.5 that an increase of a_1 would result in an increase of the inverse time scale or decrease the response time of the body. In contrast the mass ratio has the opposite effect where an increase in m^*will lead to a decrease in λ, since a heavier body (or a body with higher inertia) would have a slower response.

In order to find the relevant dimensionless groups of the problem, the time scale formulated could be used to non-dimensionalise the equation of motion. The equation of motion presented in Equation ***KJ: put final equation of motion *** can be non-dimensionalised using the non dimensional time τ, defined as $\tau = t(a_1/m^*)(U/D)$. The non-dimensional equation of motion could then be represented as,

$$\ddot{Y} + \frac{m^{*2}}{a_1^2}\frac{kD^2}{mU^2}Y = \left(\frac{1}{2} - \frac{m^*}{a_1}\frac{cD}{mU}\right)\dot{Y} - \frac{a_1 A_3}{m^{*2}}\dot{Y}^3 + \frac{a_1^3 a_5}{m^{*4}}\dot{Y}^5 - \frac{a_1^5 a_7}{m^{*6}}\dot{Y}^7. \tag{1.6}$$

The equation could be further altered by regrouping the coefficients into non-dimenasional groups and could be expressed as,

$$\ddot{Y} + \frac{4\pi^2 m^{*2}}{U^{*2}a_1^2}Y = \left(\frac{1}{2} - \frac{c^* m^*}{a_1}\right)\dot{Y} - \frac{a_1 A_3}{m^{*2}}\dot{Y}^3 + \frac{a_1^3 a_5}{m^{*4}}\dot{Y}^5 - \frac{a_1^5 a_7}{m^{*6}}\dot{Y}^7, \tag{1.7}$$

$U^*$is the reduced velocity which is the typical independent variable ussed in vortex-induced vibration studies. $c^*$is the non-dimensional damping parameter which is expressed as $c^* = cD/mU$.

By analysing equation 1.7 it is clear that five dimensionless parameters play a role in setting the response of the system. These are namely the stiffness, damping, mass ratio, the

geometry and the Reynolds number. The stiffness is repented by the reduced velocity U^*, the damping by $c^*$and the mass ratio by m^*. The geometry and the Reynolds number are represented by the coefficients a_n, of the polynomial fit to the C_y curve. Using the natural time scales of the system, grouping of these non-dimensional parameters into two groups in the non-dimensional equation of motion, suggests that there are two groups that governs the response which are: $\Gamma_1 = 4\pi^2 m^{*2}/U^{*2}a_1^2$ and $\Gamma_2 = c^* m^*/a_1$. Γ_1 could be described as a combined mass-stiffness, where Γ_2 could be expressed as a combined mass-damping parameter for a given geometry and a Reynolds number. It is assumed that the stiffness plays a minor role, Γ_2 seems more likely parameter to collapse the data. The wind tunnel data in the classic paper of galloping by (Parkinson and Smith, 1964) adopted a parameter similar to Γ_2 to collapse the data.

All of the quantities that formulate Γ_1 and Γ_2 except a_1 in theory, could be obtained before an experiment. However in order to obtain the value of a_1 static body experiments are required making it relatively difficult to obtain. Here, the $Re$and the geometry remains constant and therefore multiplying Γ_1 with ${a_1}^2$ and Γ_2 with a_1 suitable parameters could be obtained, and formulate a mass-stiffness parameter $\Pi_1 = 4\pi^2 m^{*2}/U^{*2}$, and a mass-damping parameter defined as $\Pi_2 = c^* m^*$. Therefore equation 1.7 can be written in terms of Π_1 and Π_2.

$$\ddot{Y} + \Pi_1 Y = \Pi_2 \dot{Y} - \frac{a_1 a_3}{m^{*2}}\dot{Y}^3 + \frac{a_1^3 a_5}{m^{*4}}\dot{Y}^5 - \frac{a_1^5 a_7}{m^{*6}}\dot{Y}^7, \tag{1.8}$$

From equation 1.8, it is clear that the governing parameters of the non dimensionlised equation are Π_1 $\Pi_2$and m^*. However, form closer inspection it is possible to see that m^*has an impact on the non-linear terms of the forcing function. The velocity pf the and hence the induced angle of attack needs to be very high in order for the non-linear terms to be applicable.

1.3 Quasi-steady state results

1.3.1 Classical VIV parameters vs. Π_1 and Π_2.

Vortex-induced vibrations being another form fluid-structure interaction which occurs in a slender structure, has been investigated as candidate for power extraction from external

flows. Significant progress on this problem have been made by Bernitsas et al. (2008, 2009); Raghavan and Bernitsas (2011); Lee and Bernitsas (2011) and other colleagues in VIVCACE group in the University of Michigan. Hence, it may seem that it is reasonable to present the data in a fluid-elastic problem using the same parameters in a VIV problem.

QSS data presented in figure 1.1 at $Re = 200$, shows a comparison between classical VIV and the newly formulated parameters presented as independent variables. The displacement amplitude, velocity amplitude and the mean power is presented in sub-figures (a), (c) and (e), as functions of the classical VIV parameter $U^*$for different ζ. The same data as functions of Π_2, are presented in sub-figures (b), (d) and (f), for various, reasonably high values of Π_1 ***KJ: put the parameters used section ***. Sub-figure (e) shows a similar trend to Barrero-Gil et al. (2010). The Value of the peak power remains constant. However, the power curve shifts to the right as ζ is increased. Here, in figure 1.1 the maximum dimensionless power is achieved at two times the velocity at which the galloping starts, which is similar to the observations made by Barrero-Gil et al. (2010); Vicente-Ludlam et al. (2014). An excellent collapse for velocity amplitude and mean power could be observed on the data, presented using the dimensionless group Π_2, formulated using the natural time scales of the system. This implies that essentially velocity amplitude and the mean power is dictated by $\Pi_2$which furthermore, implies that the natural frequency of the system which is used to scale U^*, ζ and $\Pi_1$does not have a significant influence on the behaviour of the system, unlike VIV, which is a resonant phenomenon.

1.3.2 High and low Re data

The successful collapse of data, mean power in particular using $\Pi_2$for low Reynolds number ($Re = 200$), could be replicated at high Reynolds numbers. An example case is presented in figure 1.1 at $Re = 22300$ for selected vales of Π_1. The successful collapse of mean power data at high Reynolds numbers shows that suitability of using Π_2 as an independent variable across a large range of Reynolds numbers.

Hysteresis is evident in the high Reynolds number case ($Re = 22300$). Manipulating the initial condition (initial displacement) lead to obtaining different solutions for the same Π_2 value. The upper and lower branch were obtained by giving an initial displacement which was higher than the expected amplitude and providing a lower initial displacement

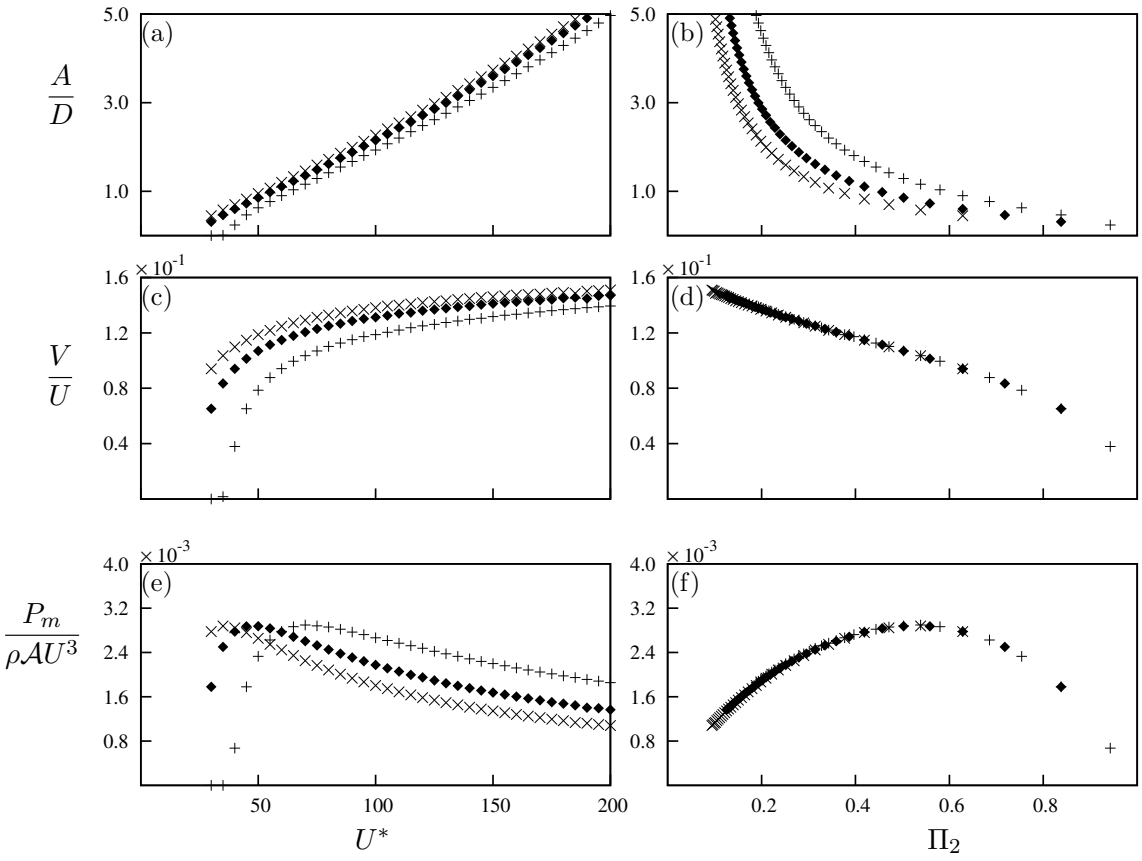

Figure 1.1: Displacement amplitude, velocity amplitude and dimensionless mean power data as functions of two different independent variables. Data presented in (a), (c) and (e) using the classical VIV parameter U^*, obtained at $Re = 200$ and $m^* = 20$ at three different damping ratios: $\zeta = 0.075$ (×), $\zeta = 0.1$ (◆) and $\zeta = 0.15$ (+). (b) (d) and (f) are the same data presented using the combined mass-damping parameter (Π_2) as the independent variable. Even though Π_1 varies in the range of $0.4 \leq \Pi_1 \leq 17.5$, it is clear that the power is a function of Π_2 only.

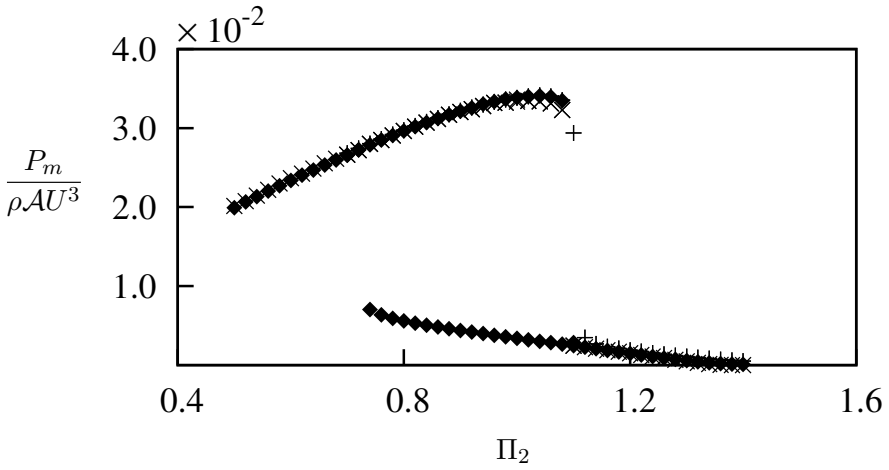

Figure 1.2: Dimensionless mean power as a function of Π_2. Data presented at (a) Re = 22300, $\Pi_1 = 200$ (×), $\Pi_1 = 2000$ (◆) and $\Pi_1 = 10000$ (+). Hysteresis could be observed at high Re.

respectively. Even though in theory, there is a possibility of a third state, this unstable branch could not be achieved with a time integration method (also observed by (Vio et al., 2007)) such as the one employed in this study.

1.3.3 Dependence on mass-stiffness, Π_1

From the results of sections 1.3.1 and 1.3.2 shows essentially a single variable governs the mean extracted power, which is the combined mass-damping parameter, Π_2. The time scale analysis carried out in section 1.2 shows that not only Π_2 but also $\Pi_1$influences the system. Previous studies such as Bouclin (1977) have also reported a complex interaction between the displacement amplitude and the natural frequency, for high natural frequencies in particular; or in this instance equivalent to low values of Π_1. This section investigates the impact of $\Pi_1$further. The overall behavior of the system is divided into two regimes, one for "high" Π_1 and the other for "low" $\Pi_1$and analysed.

The mean power as a function of Π_2 for a range of values of $\Pi_1$is presented in figure 1.3. In the two subfigures presented, (a) shows the data for $\Pi_1 \geq 10$, while (b) shows data for $\Pi_1 \leq 10$. The excellent collapse in figure 1.3(a) shows that for $\Pi_1 \geq 10$, the mean power is independent of Π_1.

In contrast figure 1.3(b) shows that for low values of $\Pi_1 \leq 10$, the predicted mean power

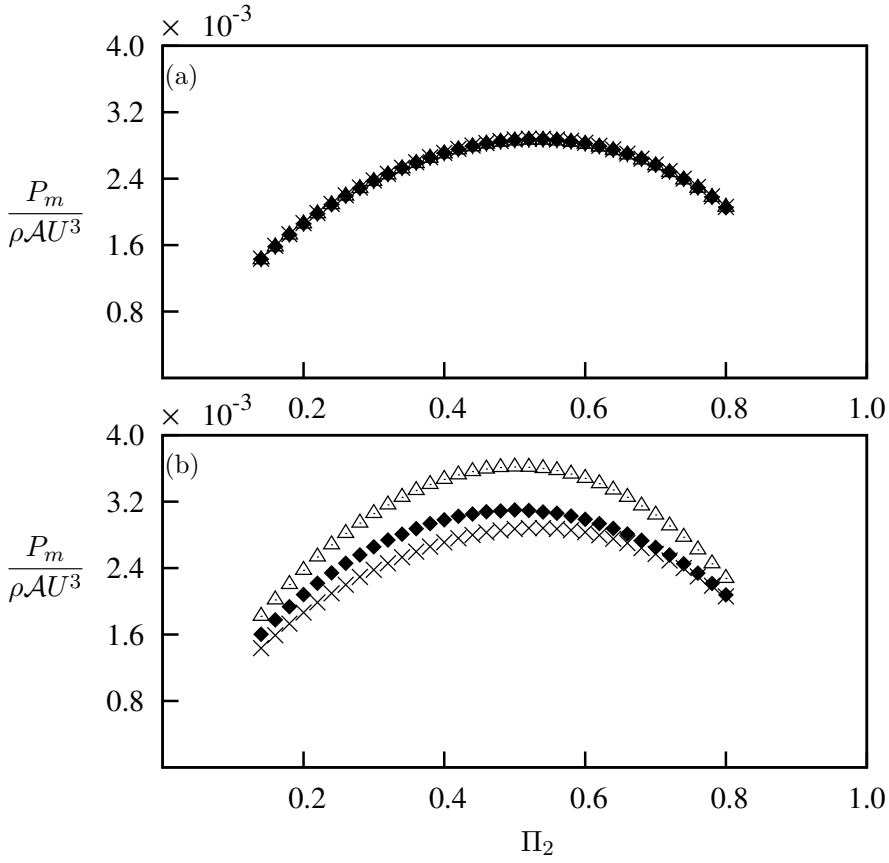

Figure 1.3: Dimensionless mean power as a function of Π_2 obtained using the QSS model at $Re = 200$. (a) High Π_1; data presented at four different combined mass-stiffness levels. $\Pi_1 = 10$ ($m^* = 20,\ U^* = 40$) (×), $\Pi_1 = 100$ ($m^* = 80,\ U^* = 50$) (+), $\Pi_1 = 500$ ($m^* = 220,\ U^* = 60$) (◆) and $\Pi_1 = 1000$ ($m^* = 400,\ U^* = 40$) (△). (b) Low Π_1; data presented at $\Pi_1 = 10$ (×), $\Pi_1 = 0.1$ (◆), and $\Pi_1 = 0.01$ (△).

increases as $\Pi_2$decreases. This indicates that at this region ($\Pi_1 < 10$), the mean power is a weak function of Π_1, hence, providing a distinction between high and low regimes of Π_1.

Bibliography

Barrero-Gil, A., Alonso, G., Sanz-Andres, A., Jul. 2010. Energy harvesting from transverse galloping. Journal of Sound and Vibration 329 (14), 2873–2883.

Bernitsas, M. M., Ben-Simon, Y., Raghavan, K., Garcia, E. M. H., 2009. The VIVACE Converter: Model Tests at High Damping and Reynolds Number Around 10[sup 5]. Journal of Offshore Mechanics and Arctic Engineering 131 (1), 011102.

Bernitsas, M. M., Raghavan, K., Ben-Simon, Y., Garcia, E. M. H., 2008. VIVACE (Vortex Induced Vibration Aquatic Clean Energy): A new concept in generation of clean and renewable energy from fluid flow. Journal of Offshore Mechanics and Arctic Engineering 130 (4), 041101–15.

Bouclin, D. N., 1977. Hydroelastic oscillations of square cylinders. Master's thesis, University of British Columbia.

Lee, J., Bernitsas, M., Nov. 2011. High-damping, high-Reynolds VIV tests for energy harnessing using the VIVACE converter. Ocean Engineering 38 (16), 1697–1712.

Parkinson, G. V., Smith, J. D., 1964. The square prism as an aeroelastic non-linear oscillator. The Quarterly Journal of Mechanics and Applied Mathematics 17 (2), 225–239.

Raghavan, K., Bernitsas, M., Apr. 2011. Experimental investigation of Reynolds number effect on vortex induced vibration of rigid circular cylinder on elastic supports. Ocean Engineering 38 (5-6), 719–731.

Vicente-Ludlam, D., Barrero-Gil, A., Velazquez, A., 2014. Optimal electromagnetic energy extraction from transverse galloping. Journal of Fluids and Structures 51, 281–291.

Vio, G., Dimitriadis, G., Cooper, J., Oct. 2007. Bifurcation analysis and limit cycle oscillation amplitude prediction methods applied to the aeroelastic galloping problem. Journal of Fluids and Structures 23 (7), 983–1011.